Inter-Comparability of Radiometric Performance between Sentinel-1A and Sentinel-1B

Kersten Schmidt[a], Marco Schwerdt[a,], Nuno Miranda[b]
[a] Microwaves and Radar Institute, German Aerospace Center (DLR), Oberpfaffenhofen, Germany
[b] ESA-ESRIN, Via Galileo Galilei, 00044 Frascati, Italy

Abstract

The study shows that Sentinel-1B is more sensitive for low backscatter due to higher TX power and higher RX pattern gain compared to Sentinel-1A. Therefore targets covering a wide backscatter range are compared. While for point targets and medium backscatter areas (e.g. rainforest) no significant radiometric differences are found, the NEBZ within calm water is lower for Sentinel-1B compared to Sentinel-1A by about 1.4 dB. By evaluating transponder recordings, the SAR transmit power is found to be higher for Sentinel-1B compared to Sentinel-1A by about 0.7 dB. These different radiometric performances are present although both SAR systems are well calibrated.

1 Introduction

Sentinel-1 is the first space-borne SAR mission in the frame of the Copernicus program for Earth Observation directed by the European Commission in partnership with ESA. The main objective of the Sentinel-1 mission is to ensure the continuity of C-band SAR data acquisitions for global monitoring applications **[1]**. The mission consists of a SAR constellation with Sentinel-1A (S-1A) and Sentinel-1B (S-1B) flying in a near-polar sun-synchronous orbit and operating a synthetic aperture radar (SAR) at C-band. Both SAR systems were independently calibrated by DLR on behalf of ESA during their commissioning phases in 2014 **[2]** and 2016 **[3]**.

Calibrated radiometric SAR products are essential for various applications and an important basis for the quality of further derived products. Accurate measured radar brightness is used to classify or even quantify the observed target area, e.g. ice area, forest or other kind of vegetation, soil moisture as well as ocean currents or wind speed.

For well calibrated products, users should expect that radiometric performance is independently from the used SAR system. However, even if SAR systems are calibrated with point targets, differences may occur for low backscattering areas due to different system noise.

2 Radiometric Performance

The current study evaluates the radiometric performance of both Sentinels (S-1A and S-1B) and analyses the comparability in terms of measured radar backscatter. Therefore point targets with a sufficient high RCS are used but also distributed targets covering a wide backscatter range: from medium SNR found in the rainforest down to low SNR at almost noise level. To achieve comparable results distributed targets were selected showing stable backscatter behaviour over time.

2.1 Point Target Evaluations

DLR's reference targets (transponder and corner reflectors) have been used to evaluate the radiometric performance of S-1A and S-1B. Within the last 2.5 years regular SAR acquisitions have been performed over the calibration field using IW mode with VV and VH polarization. These acquisitions were used for deriving the radiometric accuracy and stability of S-1A and S-1B **[4]**.

The deviations of RCS derived from SAR images and theoretical expected ones have been evaluated; the results are depicted in **Figure 1** for S-1A (top) and S-1B (bottom). While the RCS of corner reflectors can be derived from co-polarized products (VV) only, transponder RCS are evaluated for VV (red) and VH (blue) polarization.

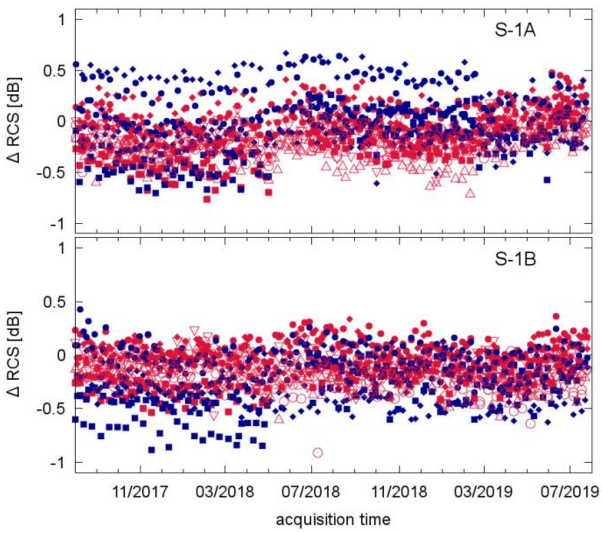

Figure 1 RCS deviation related to nominal value for DLR point targets as a function of 2.5 years observation time.

https://ieeexplore.ieee.org/document/9472561

Both SAR systems show a stable radiometric performance over time; the mean values and standard deviations are summarized in **Table 1**. Nevertheless some small “jumps” are visible within Figure 1 which are related to updates of the related SAR antenna pattern (e.g. Mar 2019 for S-1A) or a transponder maintenance (May 2018). Furthermore, seasonally related drifts are visible in particular for S-1A in the order of 0.3 dB.

Table 1 RCS deviations derived from point targets

polarization channel	S-1A RCS [dB] (μ±σ)	S-1B RCS [dB] (μ±σ)
VV	-0.19 ± 0.21	-0.11 ± 0.17
VH	-0.03 ± 0.33	-0.24 ± 0.26

2.2 Distributed Targets

In order to compare the radiometric performance between S-1A and S-1B over a wide backscatter range, distributed targets are selected which are related to different backscatter properties:

- medium SNR within the Amazon rainforest,
- transition to low SNR found in ice areas of Greenland for a wide range of incidence angle, and
- very low SNR within calm waters (Lake Constance).

2.2.1 Rainforest Area

Figure 2 depicts the footprint of three distributed targets selected as observation areas for rainforest acquisitions. The areas are spread over range and cover all three IW sub-swathes for an ascending orbit. Each rectangle contains 1000 range and 700 azimuth pixels using slantrange geometry covering areas on ground between about 28 and 32 km^2. Low spatial variation of the backscatter values are found for each target area as no disturbing features like rivers or deforested fields are located within. The IW SLC products for this ascending orbit configuration are evaluated between Sep. 2018 and Jun 2019 where dual polarization products (HH and HV) are available continuously for S-1A and S-1B.

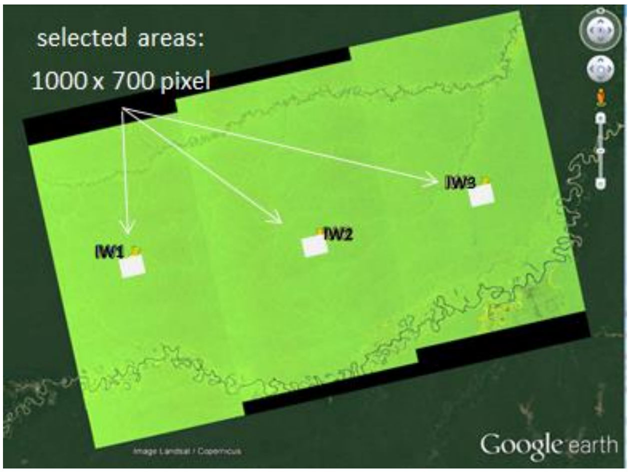

Figure 2 Three distributed targets selected within the Amazon rainforest.

2.2.2 Greenland Ice Area

For evaluating a target type with low backscatter, land ice covering the Greenland area is selected. **Figure 3** depicts the positions of five selected observation areas within this region used for the study. As seen in this figure, the backscatter is strongly related to the incidence angle which allows covering a wide range of measured radar brightness β_0 over all three IW sub-swathes. SLC products for a descending orbit configuration for the HH and HV polarization is available since September 2018.

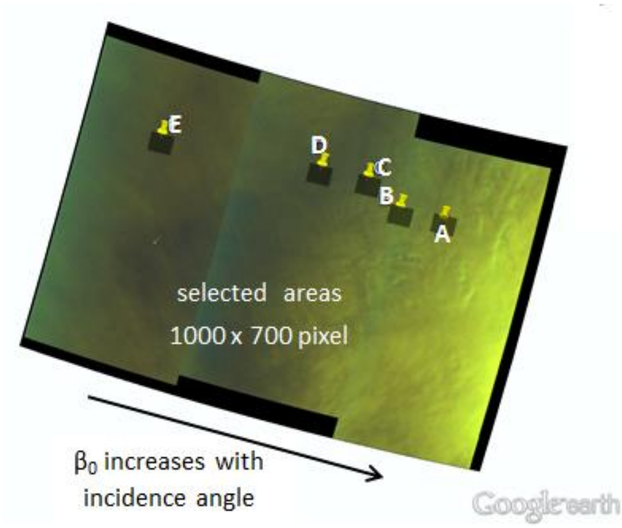

Figure 3 Five distributed targets selected within the ice area of Greenland.

2.2.3 Lake Constance

To realize a time series covering an area with very low backscatter (near noise) a distributed target within calm water is selected located at the Lake Constance (**Figure 4**). The observation area of 1000 range and 700 azimuth pixels is placed at sub-swath IW1. SLC products with VH polarization are used which are available for this configuration acquired over a long period of time continuously since Sep 2017 for both S-1A and S-1B.

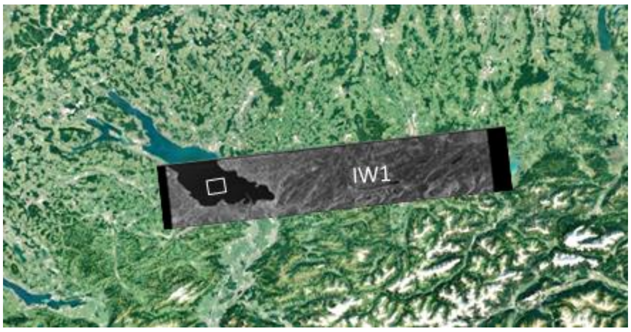

Figure 4 Distributed target (white framed) located at the Lake Constance with very low radar brightness due to calm waters.

3 Consolidating Results

The mean backscatter values and standard deviations are calculated from all observation areas shown in section 2.2. In addition the RCS evaluation from point targets are used to get a comprehensive overview about the radiometric stability of S-1A and S-1B and their inter-comparability.

For determining precisely radar brightness at low SNR, the noise level has to be taken into account by subtracting the annotated noise from the derived radar brightness in linear scale. The noise subtracted backscatter is then converted back into logarithmic scale.

3.1 Radiometric Stability

The radiometric stability is derived from the standard deviations of radar brightness from distributed targets and RCS evaluations from point targets. The results are depicted in **Figure 5**: each symbol represents a given observation area acquired with a certain incidence angle and polarization channel for S-1A and S-1B. To ensure a better comparability the same period is used for all evaluated data over a one-year observation time from Aug 2018 to Aug 2019.

As visible in **Figure 5**, the derived standard deviation depends on the target type. As expected the lowest standard deviations with values between 0.05 dB and 0.15 dB are found for the point targets. However, the distributed targets within the ice area also show low backscatter variations over time comparable to the artificial point targets. The rainforest region and also the lake area show slightly higher variations but below 0.3 dB. Furthermore, the stability measured is nearly identical for S-1A and S-1B.

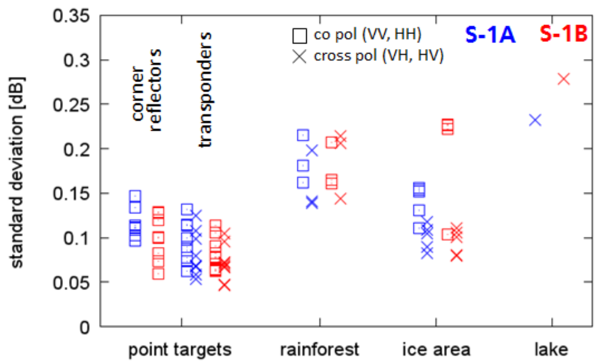

Figure 5 Standard deviations of RCS and radar brightness derived for different target types for S-1A (blue) and S-1B (red).

The investigated backscatter variations consist of contributions which are related to the SAR instruments but also to the targets and the propagation paths. The instrument stability is thought to be independent from observed targets. By considering these facts, the instrument stability is expected to be better than the lowest measured standard deviation. Hence, a recognizable instrument stability lower than 0.05 dB can be verified from these results for S-1A and S-1B.

3.2 Radiometric Inter-comparability

The radiometric comparability between S-1A and S-1B is investigated by a direct comparison between measured radar brightness over distributed targets and measured RCS derived from point targets. The results expressed as backscatter differences between S-1A and S-1B are depicted in **Figure 6** as a function of derived radar brightness for the distributed targets. Beside on the lake, the differences are below 0.6 dB. The measured RCS differences for point targets are plotted independently on the right side. These results confirm the low deviation between S-1A and S-1B mainly below 0.5 dB.

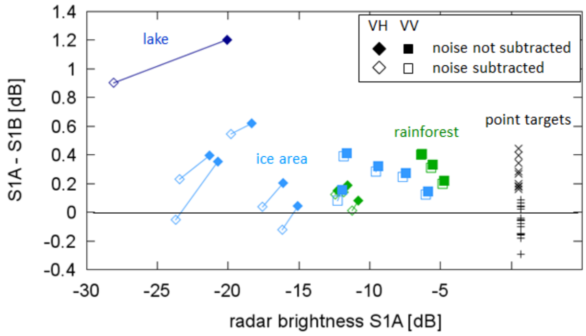

Figure 6 Radar backscatter differences between S-1A and S-1B for different target types (color) as a function of radar brightness. For low backscatter the noise subtracted values (open symbols) differ significantly from values where noise is not subtracted (full symbols).

In addition to the observed image backscatter differences between S-1A and S-1B, the noise subtracted backscatter is estimated and depicted in **Figure 6** as open symbols. Hence, by subtracting the noise, the deviation between S-1A and S-1B is further reduced. In the lake case a difference of about 0.9 dB remains which is related to a low SNR of about 1 dB for this case.

3.3 Comparing the Noise Level

As the highest deviations between S-1A and S-1B are found for very low backscatter, the noise level is further investigated. Thus the radar brightness are analysed in calm water ocean regions where a backscatter near noise is expected over a wide range covering all three IW sub-swathes.

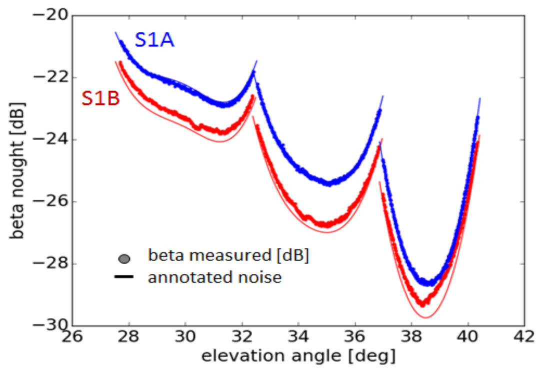

Figure 7 Radar brightness (NEBZ) over ocean regions with calm waters for IW mode VH pol.

Figure 7 depicts backscatter range profiles of one S-1A and one S-1B acquisition near the Hawaiian island as a function of radar look angle. In addition, the annotated noise profiles (lines) are plotted for both S-1A (blue) and S-1B (red). The expected noise levels match well the measured radar brightness for S-1A; for S-1B a slightly higher SNR than 0 dB seems to be present in this case.
Furthermore, it is clearly visible that S-1B reaches a lower noise equivalent beta zero (NEBZ) compared to S-1A which is also confirmed by other studies **[5]**. This difference is in average about 1.4 dB which expresses the difference between calibration factors of S-1A and S-1B. However, the found lower NEBZ values indicate a higher sensitivity of S-1B compared to S-1A related to low backscatter.

3.4 Comparing the SAR Transmit Power using Transponder Recordings

The reason for the found higher sensitivity of S-1B compared to S-1A for low backscatter could arise from a lower system noise, a higher pattern gain on receive and higher transmit power of S-1B. The latter is analysed using the ground receiver mode of DLR transponders. The transponders are able to record the signal transmitted by the SAR instrument during data acquisition. Note that these transponders are not designed for detecting an absolute power level. But by selecting data with similar transponder settings, comparisons between S-1A and S-1B overpasses with similar incidence angles are valid.
The peak power detected by the transponder is derived and the one-way free-space loss is considered. The relative power is depicted within **Figure 8** for S-1A (blue) and S-1B (red) as data points for each transponder for three different configurations (look angles). In addition, the theoretical expected gain shape from the transmit pattern of the antenna model is plotted within this figure. Note, that the profiles are shifted to match the measured power in a relative sense.

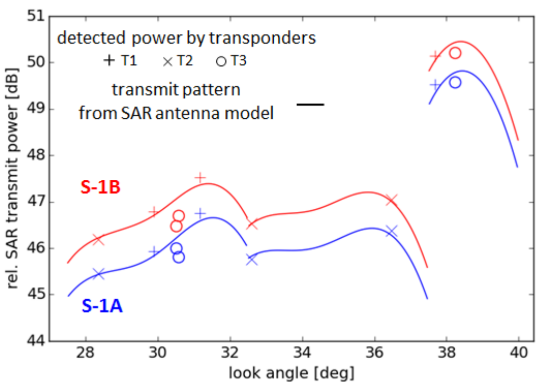

Figure 8 Relative power of transmitted SAR pulses detected by transponders (symbols) for configurations with different look angles and corresponding transmit antenna pattern (lines).

The detected power levels matches well the predicted transmit pattern from the antenna model in **Figure 8** in a relative sense. Transponder T3 shows a slightly lower power level compared to other transponders which is due to a different configuration used for this device. Furthermore, all three transponders and all three configurations show the same trend: the detected power by S-1B is higher compared to S-1A – in average by about 0.7 dB.
Based on similar two-way antenna pattern shapes provided by the antenna model for S-1A and S-1B and a 1.4 dB calibration factor difference, a higher two-way antenna gain of 1.4 dB for S-1B compared to S-1A can be deduced. As 0.7 dB are reserved by the transmit pattern, also a higher receive gain of about 0.7 dB is expected for S-1B compared to S-1A.

4 Conclusion

The radar image backscatter has been evaluated for S-1A and S-1B for different target types covering a wide backscatter range: from point targets with a high SNR over distributed targets with medium backscatter found in the rainforest down to low backscatter at ice areas and calm waters. The variation over time has been found to be target type dependent: with low standard deviation for point targets and ice areas; slightly higher values for rainforest area and calm water. From these results, a long-term instrument stability of 0.05 dB has been verified.
The radar brightness comparison shows low differences between S-1A and S-1B for point targets and medium backscatter. For targets with very low backscatter, the noise level has to be taken into account. It has been found that the detected differences for low backscatter targets arise due a higher sensitivity of S-1B for low backscatter. This higher sensitivity is expressed by a lower NEBZ visible at calm waters and a higher transmit power detected by transponders.

5 Literature

[1] Torres, R. et. al., "GMES Sentinel-1 Mission", *Remote Sensing of Environment*, (120), 9–24, **2012**.

[2] Schwerdt, M.; Schmidt, K.; Tous Ramon, N.; Castellanos Alfonzo, G.; Döring, B.; Zink, M.; Prats, P., "Independent Verification of the Sentinel-1A System Calibration", *IEEE Journal of Selected Topics in Applied Earth Observation and Remote Sensing*, 9, 994–1007, **2016**.

[3] Schwerdt, M.; Schmidt, K.; Ramon, N.T.; Klenk, P.; Yague-Martinez, N.; Prats-Iraola, P.; Zink, M.; Geudtner, D. "Independent System Calibration of Sentinel-1B", *Remote Sensing*, 9, 511, **2017**.

[4] Schmidt, K.; Tous Ramon, N.; Schwerdt, M. "Radiometric Accuracy and Stability of Sentinel-1A Determined using Point Targets", *IJMWT* (10) 538–546, **2018**.

[5] Miranda, N.; Meadows, P.; Piantanida, R.; Recchia, A.; Small, D.; Schubert, A.; Vincent, P.; Geudtner, D.; Navas-Traver, I.; Vega, F.C., "The Sentinel-1 Constellation Mission Performance," *IGARSS*, **2017**, pp. 5541–5544. doi:10.1109/IGARSS.2017.8128259.